Converging Periodic Boundary Conditions and Detection of Topological Gaps on Regular Hyperbolic Tessellations

Fabian R. Lux* and Emil Prodan†
Department of Physics and Department of Mathematical Sciences Yeshiva University, New York, New York 10016, USA

(Received 31 March 2023; revised 17 July 2023; accepted 28 September 2023; published 26 October 2023)

Tessellations of the hyperbolic spaces by regular polygons support discrete quantum and classical models with unique spectral and topological characteristics. Resolving the true bulk spectra and the thermodynamic response functions of these models requires converging periodic boundary conditions and our Letter delivers a practical and rigorous solution for this open problem on generic $\{p, q\}$-tessellations. This enables us to identify the true spectral gaps of bulk Hamiltonians and construct all but one topological models that deliver the topological gaps predicted by the K theory of the lattices. We demonstrate the emergence of the expected topological spectral flows whenever two such bulk models are deformed into each other and prove the emergence of topological channels whenever a soft physical interface is created between different topological classes of Hamiltonians.

DOI: 10.1103/PhysRevLett.131.176603

The investigation of synthetic materials is an active area of research. In particular, crystals generated from tessellations of hyperbolic spaces have been proposed and some even realized with quantum, photonic, electromagnetic, and mechanical degrees of freedom [1–6]. This is part of a new trend in materials science where the focus is shifted from making a material stronger, lighter, more durable, etc., to making it different or to behave differently. The new paradigm is geared toward creating new opportunities in materials science, which can come in the form of unique spectral characteristics or stabilization of fundamentally distinct topological phases, and the hyperbolic crystals have been a source of both [4–12]. In fact, the band topology of the hyperbolic crystals was exhaustively characterized quite a while ago [13–16].

In these endeavors, scientists are facing challenges that require entirely new tools of analysis, both theoretical and computational, and lack of such tools can hold a field hostage for years. The lack of a systematic way to impose periodic boundary conditions (PBC) on hyperbolic lattices prevents us from resolving the true bulk spectra of the Hamiltonians, computing correlations functions, bulk topological invariants, and identifying topological gaps. Since the ratio between the numbers of boundary and bulk sites converges to a strictly positive value for hyperbolic lattices, suppressing the boundary states in finite-size samples is necessary but *not* sufficient, because convergence with the sample size cannot be taken for granted. Indeed, there are many ways to fold a non-Euclidean lattice into itself and produce PBCs, but most of them do not reproduce the Green's function of the infinite lattice Hamiltonian (see Ref. [17] Sec. 5.1 and [18]).

If one is interested only in the bulk spectra, then a universal solution could be to evaluate the local density of states at or near the center of the finite-size crystal with open boundary conditions [5], but, even in the Euclidean case, this method converges only as an inverse power with the crystal size [19] and its reliability when it comes to computing thermodynamic coefficients or topological invariants is yet to be demonstrated. On the other hand, when PBCs can be systematically defined, they supply extremely fast convergences (typically exponential) with the size of the crystals, for both spectra and thermodynamic coefficients [17,20]. Partial progress on resolving the bulk characteristics of hyperbolic lattices has been achieved via generalizations of Bloch-Floquet calculus [21,22], which is intimately related to the problem of PBCs [23]. So far, these techniques can resolve the bulk spectra covered by one and two dimensional representations of the hyperbolic space groups and sometimes this seems to be just enough [5].

In our recent work [17], however, we introduced a general systematic method to impose PBCs on increasingly larger finite hyperbolic and other more general Cayley crystals, together with rigorous proofs and numerical confirmations of fast convergences to the thermodynamic limit. The folding of the infinite lattice into a finite regular graph without boundary can be achieved by taking the quotient of the hyperbolic space group with one of its finite-index normal subgroups [23–26]. To converge to the thermodynamic limit, one needs a whole coherent sequence of such normal subgroups, whose total intersection reduces to just the neutral element [24,25]. Note that, while a generic group can have a plethora of normal subgroups, only a coherent sequence can guarantee a systematic improvement of the results with system size. This is a trivial task for regular lattices in the Euclidean space, because all Euclidean space groups contain the subgroup $\mathbb{Z}^2$ of pure translations. Its normal subgroups are all

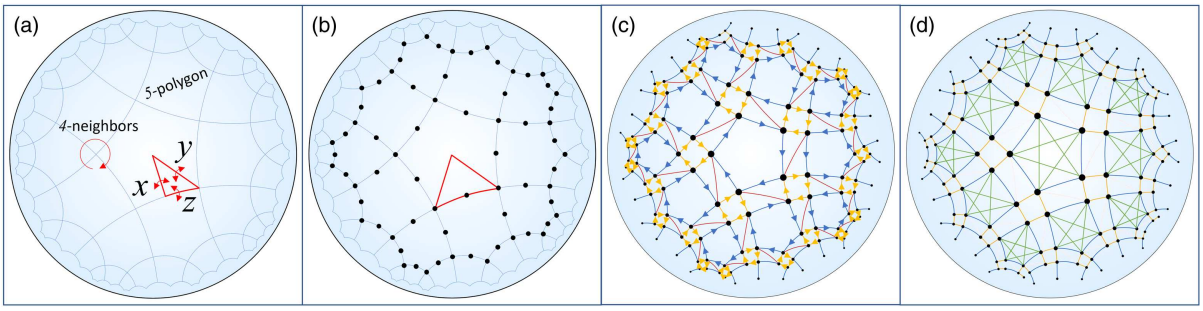

FIG. 1. (a) The $\{5,4\}$ tilling and the reflections generating the group of symmetries $\Delta_{\{p,q\}}$. (b) High symmetry points of the tilling and the fundamental domain of the proper space group $\Delta^{+}_{\{p,q\}}$. (c) The Cayley diagraph of $\Delta^{+}_{\{p,q\}}$, showing a generic symmetric lattice and the flow of the points under the right action of the generators x_1 (blue), x_2 (orange), and x_3 (red). (d) Couplings needed to implement $\pi_R[h_1(\lambda)]$ from Eq. (6), where blue $= \lambda|g\cdot x_1^{-1}\rangle\langle g| + \lambda^{-1}|g\rangle\langle g\cdot x_1^{-1}|$, green $= \lambda^2|g\cdot x_1^{-2}\rangle\langle g| + \lambda^{-2}|g\rangle\langle g\cdot x_1^{-2}|$, and orange $= |g\cdot x_2^{-1}\rangle\langle g| + |g\rangle\langle g\cdot x_2^{-1}|$. The latter is only needed for the structure's integrity.

multiples of $\mathbb{Z}^2$ and quotients by these subgroups produce finite-size approximations with PBCs that all look the same. This is not the case in the hyperbolic spaces, yet the algorithm devised in [17] does just that. To work, it requires at the input a faithful representation of the hyperbolic space group as a subgroup of $\mathrm{GL}(n,R)$ [27], where R is a ring extension of $\mathbb{Z}$. Then the quotients that supply the finite-size approximations are generated by applying ordinary mod functions on the matrix entries. Such a faithful representation was provided in [17] for the simplest hyperbolic space group. Here, we supply this input together with computer algorithms that completely solve the problem of converging PBCs on generic regular hyperbolic $\{p,q\}$ tessellations.

As an application, we show that a hyperbolic model Hamiltonian that was assumed in the literature to be spectrally gapped is actually ungapped. We also resolve all topological bands supported by a $\{p,q\}$ tessellation, except one [28], in the sense that we build gapped model Hamiltonians that display these bands at the bottom of the spectrum. Given that our numerically computed spectra are clean of boundary spectrum, we can demonstrate the main topological feature of these models, namely, the emergence of a topological spectral flow whenever a distinct pair of topological Hamiltonians are continuously deformed into each other. The topological bands are listed by the K_0 group of the space group's C^* algebra and we simply took this information from [14,16].

Let $\mathbb{D}$ be the open disk model of the hyperbolic two-dimensional space. Topologically, it is identical with the Euclidean disk, but $\mathbb{D}$ carries the metric $ds^2 = [dzd\bar{z}/(1-|z|^2)^2]$. The homeorphisms of the disk preserving this metric form the continuous group $\mathrm{Iso}(\mathbb{D})$ of hyperbolic isometries. Its discrete subgroups of orientation preserving disk transformations with compact fundamental domains are called Fuchsian groups of first kind. Up to isometries, they are classified by their signatures $\langle g;\nu_1,\ldots,\nu_r\rangle$ and can be presented via $2g+r$ generators and relations as

$$\mathcal{F}_{g,\boldsymbol{\nu}} = \langle a_1,b_1,\ldots,a_g,b_g,x_1,\ldots,x_m| \; x_1^{\nu_1},\ldots,x_m^{\nu_m}, x_1\cdots x_m[a_1,b_1]\cdots[a_g,b_g]\rangle, \quad (1)$$

where $[a,b] \coloneqq aba^{-1}b^{-1}$ denotes the commutator of two elements [[29], Ch. 2]. The tessellations of $\mathbb{D}$ by regular $\{p,q\}$ polygons are always possible if $1/p+1/q<1/2$. We will use the $\{5,4\}$ tessellation shown in Fig. 1(a) for our exemplifications. The full group of hyperbolic isometries preserving this tilling is the triangle group $\Delta_{\{5,4\}}$ generated by the three reflections x, y, z against the sides of the triangle shown in Fig. 1(a). It has a maximal subgroup of proper transformations, which is the Fuchsian group $\Delta^{+}_{\{p,q\}} = \langle 0;p,q,2\rangle$ with $x_1 = xy$, $x_2 = yz$, $x_3 = zx$ and the fundamental domain indicated in Fig. 1(b).

Tillings do not automatically come with vertices. The points that are fixed by an element of $\Delta^{+}_{\{p,q\}}$ are shown in Fig. 1(b) and a generic symmetric lattice can be generated by acting on any point of the disk that is distinct from those points of high symmetry, e.g., as shown in Fig. 1(c). Such procedure actually produces the standard Cayley diagraph of $\Delta^{+}_{\{p,q\}}$, which encodes the entire group-algebraic information in a geometric fashion [30]. Our tight-binding Hamiltonians are defined on the lattice $\mathcal{L}$ from Fig. 1(c), whose points are labeled by the elements of $\Delta^{+}_{\{p,q\}}$. *All* symmetric Hamiltonians are generated from the group algebra $\mathbb{C}\Delta^{+}_{\{p,q\}}$ [31]. Concretely, $\Delta^{+}_{\{p,q\}}$ acts via the left-regular representation $\pi_L(g)|g'\rangle = |gg'\rangle$ on the Hilbert space $\ell^2(\mathcal{L})$ spanned by the vectors $|g\rangle$, $g\in\Delta^{+}_{\{p,q\}}$, while the Hamiltonians

$$h = \sum_g w_g\cdot g \in \mathbb{C}\Delta^{+}_{\{p,q\}}, \quad w_g = w^*_{g^{-1}} \in \mathbb{C} \quad (2)$$

act via the right-regular representation of $\mathbb{C}\Delta^{+}_{\{p,q\}}$,

$$H = \pi_R(h), \qquad H|g'\rangle = \sum_g w_g |g' g^{-1}\rangle. \tag{3}$$

Then $[\pi_L(g), \pi_R(h)] = 0$ can be manually checked.

We now explain Lück's work [24,25] on formulating PBCs in algebraic fashion. Any finite-index normal subgroup N_k of $\Delta^+_{\{p,q\}}$ sets a canonical projection onto the finite quotient subgroup, $\rho_k\colon \Delta^+_{\{p,q\}} \to G_k = \Delta^+_{\{p,q\}}/N_k$, which can be lifted to the level of group algebras:

$$h \mapsto \rho_k(h) = \sum_g w_g \cdot \rho_k(g) \in \mathbb{C}G_k. \tag{4}$$

As before, the right-regular representation π_R of $\mathbb{C}G_k$ acts on the Hilbert space $\ell^2(G_k)$ spanned by $|g_k\rangle$, $g_k \in G_k$. This is a finite Hilbert space of dimension $|G_k|$ (= the order of G_k) and, as such, $\rho_k(H) = \pi_R[\rho_k(h)]$ is a finite-size approximation of H. According to Lück [24,25], to achieve the thermodynamic limit, one needs a whole coherent sequence of normal subgroups $\Delta^+_{\{p,q\}} = N_0 \rhd N_1 \rhd N_2 \cdots$, such that $\cap N_k = \{1\}$, in which case the Green's functions can be recovered with arbitrary precision from the so-constructed finite-size approximations

$$\langle g|(H-z)^{-1}|g'\rangle = \lim_{k\to\infty} \langle \rho_k(g)|(\rho_k(H)-z)^{-1}|\rho_k(g')\rangle.$$

This in turn assures that the spectrum, thermodynamic coefficients, correlation functions, topological invariants, etc., can be computed with arbitrary precision from the so-constructed finite-size approximations.

Reference [17] observed that the maps ρ_k can be as straightforward as applying the modulo arithmetic operator on certain coefficients, if N_k's are generated in a specific way. Following the same strategy and by referring to Coxeter group theory [32–35], we found systematic representations of $\Delta^+_{\{p,q\}}$ in $\mathrm{SL}(3, \mathbb{Z}[\xi])$, the special linear group of 3×3 matrices with entries from the ring extension $\mathbb{Z}[\xi]$, where $\xi = 2\cos(\pi/pq)$ (see Eqs. (13)–(15) in [18]). The coherent sequence of subgroups can then be simply taken as $N_k = \Delta^+_{\{p,q\}} \cap \mathrm{SL}(3, s^k\mathbb{Z}[\xi])$, $s, k \in \mathbb{N}$. The quotient groups G_k by these N_k's can be computed as follows. First, ξ is a root of a minimal irreducible polynomial of degree $\varphi(2pq)/2$, where φ is Euler's totient function [36,37]. Thus, every entry in the matrix representations of $\Delta^+_{\{p,q\}}$ can be written as $\sum_{r=0}^{\varphi/2-1} c_r \xi^r$, with $c_r \in \mathbb{Z}$ [38]. Ordinary multiplication of such series followed by the algebraic reduction leads to a specific multiplication of the coefficients $\boldsymbol{c} = \{c_r\}$, which we denote by $\boldsymbol{c} \star \boldsymbol{c}'$ (see Ref. [18] for full details). Then G_k is the image in the finite group $\mathrm{SL}(3, \mathbb{Z}_{s^k}[\xi])$ of the elements of $\Delta^+_{\{p,q\}}$ under taking the mod s^k operation on the coefficients c_r. Thus, every entry of these matrices can be written as $\sum_{r=0}^{\varphi/2-1} \tilde{c}_r \xi^r$, with $\tilde{c}_r \in \mathbb{Z}_{s^k}$. As for the multiplication in $G_k \subset \mathrm{SL}(3, \mathbb{Z}_{s^k}[\xi])$, it is the usual matrix multiplication but with the multiplication of the entries replaced by

$$\left(\sum_{r=0}^{\varphi/2-1} \tilde{c}_r \xi^r\right) \cdot \left(\sum_{r=0}^{\varphi/2-1} \tilde{c}'_r \xi^r\right) = \sum_{r=0}^{\varphi/2-1} (\tilde{\boldsymbol{c}} \star \tilde{\boldsymbol{c}}')_r \mod s^k \xi^r.$$

With these in place, the $\rho_k(g)$'s seen in Eq. (4) are calculated by applying mod s^k on the matrix representations of g's. The approximated Hamiltonian $\rho_k(H)$ acts on $\ell^2(G_k)$ via the right-regular representation, which works as in Eq. (3) with $\Delta^+_{\{p,q\}}$ replaced by G_k. Numerically, this requires an indexing of the elements of G_k and the computation of its multiplication table, which are both straightforward tasks at this point.

A full working code implementing all the above can be downloaded from [39]. It can be seen in action in Fig. 2(a), where the bulk spectrum of the adjacency operator $\Delta = \frac{1}{4}(x_1 + x_1^{-1} + x_2 + x_2^{-1})$ is resolved and the exponentially fast convergence to the thermodynamic limit is demonstrated. In Fig. 2(b), we show the integrated density of states (IDS) computed with open boundary conditions for

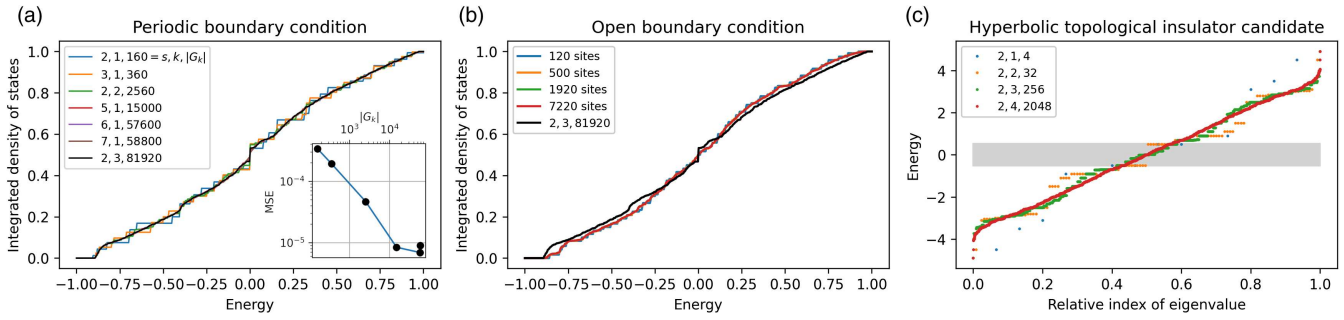

FIG. 2. (a) Integrated density of states (IDS) of the adjacency operator Δ as function of energy and finite sizes. The inset shows the mean squared error with the largest system as reference. (b) IDS of Δ with open boundary condition for various system sizes, compared to periodic boundary conditions (black curve). (c) IDS of the Hamiltonian considered in Ref. [6] for different system sizes with PBCs, showing the topological gap predicted by the $U(1)$-hyperbolic Bloch band theory (gray zone) filling in with non-Abelian states in the thermodynamic limit.

increasing lattice sizes. A comparison with the "exact" IDS from panel (a) reveals convergence to an incorrect thermodynamic limit. Lastly, in Fig. 2(c), we report a computation for the model on the $\{8,8\}$ tessellation considered in [6], which is mapped into the strong A-class topological insulator on $\mathbb{Z}^4$ lattice [40] [p. 31] by the hyperbolic $U(1)$-band theory (see Ref. [18] for full details). It is tempting to infer that this hyperbolic model has a topological gap that carries a second Chern number. However, while this model displays a gap for small lattice sizes, the exact thermodynamic limit of the IDS is gapless. Also, the known K-theoretic groups (see below) do not afford a second Chern number [13–16]. As observed in [6], the assumptions behind hyperbolic $U(1)$-band theory are not generally met and now we can confirm that this is the case for the Hamiltonian simulated in Fig. 2(c).

We now resolve the topological bands supported by the $\{p,q\}$ tessellations. As we have already seen, the symmetric Hamiltonians live inside the C^* algebra of the space group. For a generic $\mathcal{F}_{g,\boldsymbol{\mu}}$ as in Eq. (1), the K_0 group of this algebra is isomorphic to $\mathbb{Z}^{2+\sum_{\alpha=1}^{m}(\nu_\alpha-1)}$ [41]. It is freely generated by the identity, a projection p_0 that carries the hyperbolic 1st-Chern number [13–15] and by the spectral projections of the cyclic elements x_α,

$$p_\alpha(\lambda_k)=\frac{1}{\nu_\alpha}\sum_{j=0}^{\nu_\alpha-1}\lambda_k^j x_\alpha^j,\qquad \lambda_k=e^{\frac{2\pi ik}{\nu_\alpha}},\qquad k=\overline{1,\nu_\alpha}. \tag{5}$$

This assures us that any band projection of a symmetric Hamiltonian can be continuously deformed into a stacking of these fundamental projections $p_0^{n_0}\oplus p_1(\lambda_1)^{n_1(\lambda_1)}\oplus\cdots\oplus p_m(\lambda_{\nu_m})^{n_m(\lambda_{\nu_m})}$ without closing the flanking spectral gaps [42]. The integer numbers $\{n_0,n_1(\lambda_1)\ldots,n_m(\lambda_{\nu_m})\}$ represent a complete set of independent topological invariants of a band [40].

In the case of $\Delta^+_{\{p,q\}}=\langle 0;p,q,2\rangle$, we have a total of eight $p_\alpha(\lambda)$ projections and, for example,

$$h_\alpha(\lambda,\epsilon)=\epsilon\big(1-2p_\alpha(\lambda)\big)+(1-\epsilon)\Delta \tag{6}$$

are model Hamiltonians displaying topological bulk gaps and bottom spectral bands carrying the K-theoretic labels $n_\alpha(\lambda)=1$ [43]. The openings of these topological spectral gap are shown in Fig. 3 and the physical couplings needed to implement $h_1(\lambda)$ are shown in Fig. 1(d). Figure 4(a) demonstrates the distinct topological characters of the models (6), by sampling the energy spectra resulted from pairwise interpolations. The seen topological spectral flows, which actually occur for any possible pair, demonstrate that two such models cannot be adiabatically connected. Since these topological spectral flows are stable against turning on or off degrees of freedom, they can be used in applications that require robust spectral

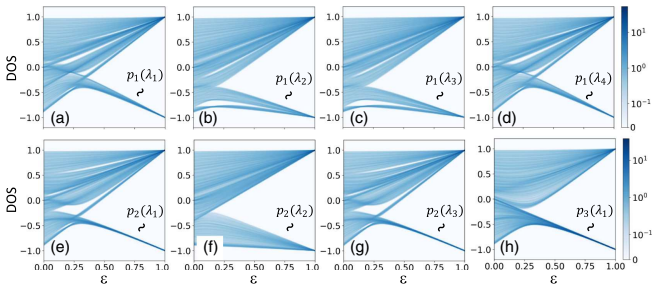

FIG. 3. Opening available topological gaps using the model Hamiltonians (6). The topological classes of the lower bands are specified in each panel, where $\lambda_j=e^{(\imath 2\pi j/\nu_\alpha)}$. The calculations are performed with PBC generated by $(s,k)=(2,3)$.

engineering. Witnessing these topological spectral flows would have been impossible without PBCs.

Another application is engineering soft topological interface channels, which can be achieved by rendering the smooth interpolations from Fig. 4(a) in space. Because of the large number of available topological phases, we can engineer complex interfaces such as the Y junction shown in Figs. 4(b)–4(d). There, we use the smooth partition of the hyperbolic unit disk $\sum_{i=1}^{3}\chi_i(z)=1$ shown in Fig. 4(b), and generate a Hamiltonian H with matrix elements

$$\langle z|H|z'\rangle=\sum_{i=1}^{3}\chi_i(\mu_{z,z'})\langle z|H_i|z'\rangle,\qquad z,z'\in\mathcal{L}, \tag{7}$$

where $\mu_{z,z'}$ is the mid geodesic point of z and z' [44]. It smoothly interpolates in space between the Hamiltonians H_1, H_2, H_3 showcased in Figs. 3(a),3(e), and 3(h), respectively. Figure 4(c) shows renderings of the local density of states

$$\mathrm{LDOS}(E,z)=\sum_n e^{-|E_n-E|^2/(2\Delta E^2)}|\psi_n(z)|^2, \tag{8}$$

for several values of ΔE, where the sum is over the eigenstates $H|\psi_n\rangle=E_n|\psi_n\rangle$. The energy E is pinned at

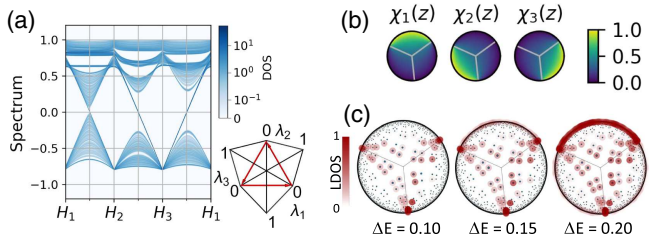

FIG. 4. (a) Energy spectrum of the Hamiltonian $\lambda_1H_1+\lambda_2H_2+\lambda_3H_3$ along the path shown in the inset, as computed with the PBC $(s,k)=(2,3)$ and with H_i as in Fig. 3 panels (a), (e), (h), respectively, and $\epsilon=0.8$. (b) Our smooth partition system for the hyperbolic disk. (c) Local density of states (LDOS) (8) of Hamiltonian (7), as computed with open boundary conditions on a crystal with 14 255 sites.

$E = 0$ in the middle of the common bulk gap of the Hamiltonians H_i's, and where Fig. 4(a) shows a crossing of topological modes. The plots in Fig. 4(c), generated with the kernel polynomial method [45], confirm the expected soft topological interface modes between the distinct topological phase.

In conclusion, we derived an algorithmic procedure to impose PBCs on finite hyperbolic crystals of increasing sizes and demonstrated the exponentially fast convergence of the bulk properties to the thermodynamic limit when computed with our algorithms. Our Letter enables now the identification of the gapped topological phases supported by generic $\{p, q\}$ tessellations of the hyperbolic spaces and simulations of various topological dynamical effects. Work is in progress on how to extend these results in the presence of a magnetic field.

Note added.—After submission of this Letter, we became aware of the works [46,47] on the same subject. The method developed in [46] covers only tight-binding Hamiltonians with uniform hopping coefficients, which can be attacked by combinatorial methods, and has nothing to say about the general models treated in our Letter. The one developed in [47] seems to be inspired by the principles stated in our Letter, but the folding of the lattices uses a different algorithm that produces nicer supercells. Our method is more analytical and does not require external resources, such as the GAP package.

This work was supported by the U.S. National Science Foundation through Grants No. DMR-1823800 and No. CMMI-2131760, and from the U.S. Army Research Office through Contract No. W911NF-23-1-0127.

*Corresponding author: fabian.lux@yu.edu
†Corresponding author: prodan@yu.edu

[1] M. Ruzzene, E. Prodan, and C. Prodan, Dynamics of elastic hyperbolic lattices, Extreme Mech. Lett. **49**, 101491 (2021).
[2] A. J. Kollár, M. Fitzpatrick, and A. A. Houck, Hyperbolic lattices in circuit quantum electrodynamics, Nature (London) **571**, 45 (2019).
[3] P. M. Lenggenhager *et al.*, Simulating hyperbolic space on a circuit board, Nat. Commun. **13**, 4373 (2022).
[4] W. Zhang, H. Yuan, N. Sun, H. Sun, and X. Zhang, Observation of novel topological states in hyperbolic lattices, Nat. Commun. **13**, 2937 (2022).
[5] A. Chen, H. Brand, T. Helbig, T. Hofmann, S. Imhof, A. Fritzsche, T. Kiebling, A. Stegmaier, L. K. Upreti, T. Neupert, T. Bzdušek, M. Greiter, R. Thomale, and I. Boettcher, Hyperbolic matter in electrical circuits with tunable complex phases, Nat. Commun. **14**, 622 (2023).
[6] W. Zhang, F. Di, X. Zheng, H. Sun, and X. Zhang, Hyperbolic band topology with non-trivial second Chern numbers, Nat. Commun. **14**, 1083 (2023).
[7] Y.-L. Tao and Y. Xu, Higher-order topological hyperbolic lattices, Phys. Rev. B **107**, 184201 (2023).
[8] V. Mathai and G. C. Thiang, Topological phases on the hyperbolic plane: fractional bulk-boundary correspondence, Adv. Theor. Math. Phys. **23**, 803 (2019).
[9] A. J. Kollár, M. Fitzpatrick, P. Sarnak, and A. A. Houck, Line-graph lattices: Euclidean and non-Euclidean flat bands, and implementations in circuit quantum electrodynamics, Commun. Math. Phys. **376**, 1909 (2020).
[10] A. Comtet, On the Landau levels on the hyperbolic plane, Ann. Phys. (N.Y.) **173**, 185 (1987).
[11] D. M. Urwyler, P. M. Lenggenhager, I. Boettcher, R. Thomale, T. Neupert, and T. Bzdušek, Hyperbolic topological band insulators, Phys. Rev. Lett. **129**, 246402 (2022).
[12] Z.-R. Liu, C.-B. Hua, T. Peng, R. Chen, and B. Zhou, Higher-order topological insulators in hyperbolic lattices, Phys. Rev. B **107**, 125302 (2023).
[13] A. L. Carey, K. C. Hannabuss, V. Mathai, and P. McCann, Quantum Hall effect on the hyperbolic plane, Commun. Math. Phys. **190**, 629 (1998).
[14] M. Marcolli and V. Mathai, Twisted index theory on good orbifolds, I: Noncommutative Bloch theory, Commun. Contemp. Math. **01**, 553 (1999).
[15] M. Marcolli and V. Mathai, Twisted index theory on good orbifolds, II: Fractional quantum numbers, Commun. Math. Phys. **217**, 55 (2001).
[16] W. Lück and R. Stamm, Computations of K- and L-theory of cocompact planar groups, K-theory **21**, 249 (2000).
[17] F. R. Lux and E. Prodan, Spectral and combinatorial aspects of Cayley-crystals, Ann. Henri Poincaré (2023).
[18] See Supplemental Material at http://link.aps.org/supplemental/10.1103/PhysRevLett.131.176603 for details proofs of technical statements.
[19] D. Massatt, M. Luskin, and C. Ortner, Electronic density of states for incommensurate layers, Multiscale Model. Simul. **15**, 476 (2017).
[20] E. Prodan, *A Computational Non-Commutative Geometry Program for Disordered Topological Insulators* (Springer, Berlin, 2017).
[21] J. Maciejko and S. Rayan, Hyperbolic band theory, Sci. Adv. **7**, eabe9170 (2021).
[22] N. Cheng, F. Serafin, J. McInerney, Z. Rocklin, K. Sun, and X. Mao, Theory and boundary modes of high-dimensional representations of infinite hyperbolic lattices, Phys. Rev. Lett. **129**, 088002 (2022).
[23] J. Maciejko and S. Rayan, Automorphic Bloch theorems for hyperbolic lattices, Proc. Natl. Acad. Sci. U.S.A. **119**, e2116869119 (2022).
[24] W. Lück, Approximating L^2-invariants by their finite-dimensional analogues, Geom. Funct. Anal. **4**, 455 (1994).
[25] W. Lück, L^2-Invariants: Theory and Applications to Geometry and K-Theory, *Ergebnisse der Mathematik und ihrer Grenzgebiete*, 3. Vol. 44 (Springer-Verlag, Berlin, 2002).
[26] F. Sausset and G. Tarjus, Periodic boundary conditions on the pseudosphere, J. Phys. A **40**, 12873 (2007).
[27] $\mathrm{GL}(n, R)$ is the group of invertible $n \times n$ matrices with entries from the ring R.
[28] The band carrying the hyperbolic Chern number will be resolved in a separate study.

[29] S. Katok, *Fuchsian Groups* (University of Chicago Press, Chicago, 1992).
[30] H. S. M. Coxeter and W. O. J. Moser, *Generators and Relations for Discrete Groups* (Springer, Berlin, 1972).
[31] For a discrete group G, the group algebra $\mathbb{C}G$ consists of formal sums $\sum_{g\in G}\alpha_g \cdot g$ where only a finite number of the complex coefficients α_g are nonzero.
[32] J. E. Humphreys, *Reflection Groups and Coxeter Groups* (Cambridge University Press, Cambridge, England, 1990).
[33] J. Mennicke, Eine Bemerkung über Fuchssche Gruppen, Inventiones Mathematicae **2**, 301 (1967).
[34] J. Širáň, The triangle group representations and their applications to graphs and maps, Discrete Math. **229**, 341 (2001).
[35] J. Širáň, The triangle group representations and constructions of regular maps, Proc. London Math. Soc. **82**, 513 (2001).
[36] D. Lehmer, A note on trigonometric algebraic numbers, Am. Math. Mon. **40**, 165 (1933).
[37] W. Watkins and J. Zeitlin, The minimal polynomial of $\cos(2\pi/n)$, Am. Math. Mon. **100**, 471 (1993).
[38] This is because $\xi^{\varphi/2}$ can be expressed in terms of its lower powers. This process is referred to as algebraic reduction.
[39] https://github.com/luxfabian/hyperbolic_crystals.
[40] E. Prodan and H. Schulz-Baldes, *Bulk and Boundary Invariants for Complex Topological Insulators: From K-Theory to Physics* (Springer, Berlin, 2016).
[41] As for the ordinary topological insulators, K_0 group enumerates the class-A topological phases over the hyperbolic lattice.
[42] Degrees of freedom can be turned on or off during these continuous deformations.
[43] Model Hamiltonians delivering topological bands with $n_0 = 1$ appeared already in [11].
[44] G. Wang, M. Vuorinen, and X. Xhang, On cyclic quadrilaterals in euclidean and hyperbolic geometries, Publ. Math. Debrecen **99**, 123 (2021).
[45] A. Weiße, G. Wellein, A. Alvermann, and H. Fehske, The kernel polynomial method, Rev. Mod. Phys. **78**, 275 (2006).
[46] R. Mosseri and J. Vidal, Density of states of tight-binding models in the hyperbolic plane, Phys. Rev. B **108**, 035154 (2023).
[47] P. M. Lenggenhager, J. Maciejko, and T. Bzdušek, Non-Abelian hyperbolic band theory from supercells, arXiv: 2305.04945.